Article

Dual action of ketamine confines addiction liability

https://doi.org/10.1038/s41586-022-04993-7

Received: 10 December 2021

Accepted: 17 June 2022

Published online: 27 July 2022

Check for updates

Linda D. Simmler[1,3], Yue Li[1,3], Lotfi C. Hadjas[1], Agnès Hiver[1], Ruud van Zessen[1] & Christian Lüscher[1,2]✉

Ketamine is used clinically as an anaesthetic and a fast-acting antidepressant, and recreationally for its dissociative properties, raising concerns of addiction as a possible side effect. Addictive drugs such as cocaine increase the levels of dopamine in the nucleus accumbens. This facilitates synaptic plasticity in the mesolimbic system, which causes behavioural adaptations and eventually drives the transition to compulsion[1–4]. The addiction liability of ketamine is a matter of much debate, in part because of its complex pharmacology that among several targets includes *N*-methyl-D-aspartic acid (NMDA) receptor (NMDAR) antagonism[5,6]. Here we show that ketamine does not induce the synaptic plasticity that is typically observed with addictive drugs in mice, despite eliciting robust dopamine transients in the nucleus accumbens. Ketamine nevertheless supported reinforcement through the disinhibition of dopamine neurons in the ventral tegmental area (VTA). This effect was mediated by NMDAR antagonism in GABA (γ-aminobutyric acid) neurons of the VTA, but was quickly terminated by type-2 dopamine receptors on dopamine neurons. The rapid off-kinetics of the dopamine transients along with the NMDAR antagonism precluded the induction of synaptic plasticity in the VTA and the nucleus accumbens, and did not elicit locomotor sensitization or uncontrolled self-administration. In summary, the dual action of ketamine leads to a unique constellation of dopamine-driven positive reinforcement, but low addiction liability.

Ketamine is a club drug that is classified as a schedule III substance by the US Food and Drug Administration, and as a class B drug in the UK, owing to its putative addiction liability. Although at present it is rarely used as an anaesthetic, the debate as to what extent ketamine can cause a loss of control and compulsion has re-emerged now that the molecule is more widely used as a fast-acting antidepressant. Studies in rodents suggest that ketamine presents a risk for addiction because early microdialysis experiments revealed that it induces a general increase of dopamine in the nucleus accumbens (NAc)[7–9] — a hallmark of addictive drugs, including cocaine[4]. Moreover, behavioural studies suggest that ketamine is rewarding and reinforcing in rats[10–13], another characteristic that it has in common with addictive drugs. Ketamine has many pharmacological targets[6], among which it has the highest affinity for NMDARs (antagonist)[5]. The long-term effects of ketamine on mesolimbic reward circuits and behaviour, however, remain elusive. For example, we do not know whether ketamine induces the synaptic plasticity that is typically evoked by addictive drugs, which drives early adaptive behaviour and eventually compulsion[14,15]. A single first dose of cocaine potentiates glutamatergic synapses onto dopamine neurons in the VTA (ref. [16]), expressed by the insertion of Ca^{2+}-permeable α-amino-3-hydroxy-5-methyl-4-isoxazolepropionic acid (AMPA) receptors (AMPARs)[17,18]. This redistribution of receptors in the VTA serves as a permissive metaplasticity that, with repeated drug exposure, is reflected in a strengthening of excitatory synapses onto type-1 dopamine receptor (D_1R)-expressing medium spiny neurons (D1-MSNs) in the NAc[19–21], and eventually synaptic plasticity in the dorsal striatum[22]. Here we use latest-generation fluorescent markers and activity indicators to investigate whether ketamine increases mesolimbic dopamine, and to assess its effects on synapses and behaviour.

Reinforcement and dopamine increase in the NAc

In an open field, a single dose of 30 mg kg^{-1} ketamine enhanced locomotion similarly to a dose of cocaine (15 mg kg^{-1}; Fig. 1a,b). We next tested the rewarding and reinforcing properties of ketamine (Fig. 1c). Mice readily self-administered the drug (1 mg per kg per infusion in a 2-h short access protocol), taking a comparable number of infusions to that of cocaine (0.75 mg per kg per infusion; Fig. 1d,e and Extended Data Fig. 1). Given this behavioural hallmark, we measured dopamine using a genetically encoded dopamine sensor (dLight1.1; Fig.1f). A single intraperitoneal injection of ketamine elicited dopamine transients in the NAc that were similar in magnitude, but of shorter duration, than those elicited by cocaine (Fig. 1g). The area under the curve (AUC) of the dopamine transients increased in a dose-dependent manner (Extended Data Fig. 2).

Disinhibition of VTA dopamine neurons

To test the effects of ketamine on neuronal activity, we monitored the fluorescence of a genetically encoded Ca^{2+} sensor (GCaMP6m; Fig. 2a)

[1]Department of Basic Neurosciences, University of Geneva, Geneva, Switzerland. [2]Service de Neurologie, Department of Clinical Neurosciences, Geneva University Hospital, Geneva, Switzerland. [3]These authors contributed equally: Linda D. Simmler, Yue Li. ✉e-mail: christian.luscher@unige.ch

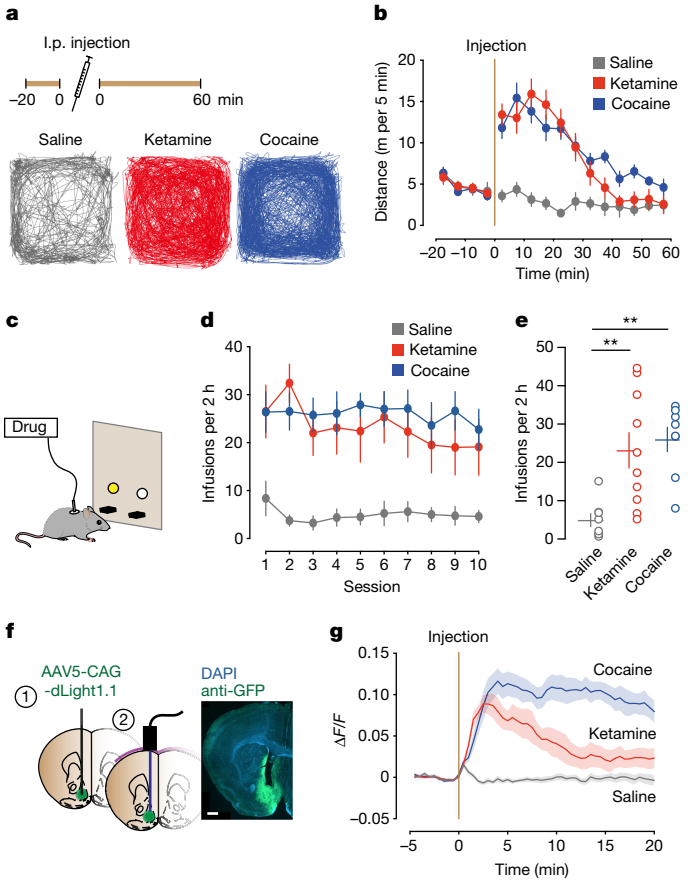

Fig. 1 | Ketamine causes hyperlocomotion, reinforcement and increased dopamine in the NAc. a, Top, experimental timeline. Bottom, representative track plots after intraperitoneal (i.p.) injections. **b**, Distance travelled before and after i.p. injections. *n* (mice) = 7 (saline), 11 (ketamine) and 11 (cocaine). **c**, Schematic of self-administration apparatus. **d**, Number of infusions in 2 h across the 10 sessions taken by mice self-administering saline, ketamine (1 mg per kg per infusion) or cocaine (0.75 mg per kg per infusion). *n* (mice) = 8 (saline), 10 (ketamine) and 8 (cocaine). **e**, Number of infusions averaged across the 10 self-administration sessions. *n* (mice) = 8 (saline), 10 (ketamine) and 8 (cocaine). **f**, Left, schematic of virus injection and fibre implantation. Right, representative picture of dLight expression. Scale bar, 500 µm. **g**, Average NAc dLight response to i.p. injections. *n* = 12 mice. Data are mean ± s.e.m. $^{**}P < 0.01$. For all i.p. injections, doses were 30 mg kg^{-1} ketamine and 15 mg kg^{-1} cocaine.

in dopamine and GABA neurons of the VTA. Intraperitoneal injection of ketamine led to an increase in the activity of dopamine neurons for 5 min (Fig. 2b), consistent with the fast kinetics that were observed for dopamine release in the NAc (Fig. 1g). By contrast, and as expected, cocaine decreased the activity of dopamine neurons in the VTA (Fig. 2b), owing to the activation of inhibitory D_2 autoreceptors[23]. In VTA GABA neurons, we observed that ketamine induced a strong and sustained inhibition (Fig. 2c), whereas cocaine did not affect the activity of these neurons. This suggests that ketamine induces a primary inhibition of VTA GABA neurons that may cause a disinhibition, but raises the question of why GCaMP6m signals in VTA dopamine neurons and dLight signals in the NAc show a short-lived change after the injection of ketamine.

We first assessed whether NMDARs expressed on GABA cells in the VTA are indeed the primary targets of ketamine. We removed the NMDARs by deleting the obligatory subunit NR1 (*Grin1*) selectively from VTA GABA cells (Fig. 2d; validated by decreased NMDA/AMPA ratios, see Extended Data Fig. 3) using a Cre-dependent CRISPR–SaCas9 knock-out (KO) strategy[24] in VGat-Cre mice. This led to the loss of the effect of ketamine on the activity of VTA GABA neurons (Fig. 2e), but did not affect fentanyl-induced GABA inhibition (Extended Data Fig. 4a,b). As a result, the ketamine-evoked release of dopamine in the NAc in VTA-GABA NR1-KO mice was reduced (Fig. 2f,g). The deletion of NMDARs in GABA neurons had also a small effect on cocaine-elicited dopamine transients (Extended Data Fig. 4e–g), possibly because of an enhanced baseline activity of dopamine neurons. The disinhibitory motif of the circuit effects of ketamine is further supported by the effect of ketamine on optogenetic inhibition of VTA GABA neurons, which is also reinforcing[25]. To this end, we expressed the inhibitory opsin eArch3.0 in VTA GABA neurons and measured dopamine transients in the NAc (Fig. 2h,i). We delivered 30 laser pulses of 10-s duration on the first day and injected a dose of ketamine (45 mg kg^{-1}) intraperitoneally after the first 5 pulses on the second day (Fig. 2i). We observed that the laser-induced dopamine transients in the NAc became smaller with ketamine treatment (Fig. 2j). This partial occlusion of laser-induced disinhibition through a non-saturating dose of ketamine corroborates the VTA-specific disinhibitory motif for the action of ketamine on the dopamine system.

We next addressed the decay kinetics in dopamine neurons despite continued inhibition of VTA GABA neurons (Fig. 2c). Ketamine-evoked dopamine transients (Fig. 1g) and dopamine neuron activity (Fig. 2b) decayed within minutes. This is in contrast to fentanyl, which caused a long-lasting, only slowly decaying NAc dopamine transient through disinhibition (Extended Data Fig. 4a–d). To investigate possible additional inhibitory mechanisms, we monitored the activity of dopamine neurons after treatment with fluphenazine-*N*-mustard (FNM; Fig. 3a,b). This irreversible D_2R antagonist extended the activity of dopamine neurons in response to ketamine (Fig. 3c) and also reduced the cocaine-induced auto-inhibition of dopamine neurons (Fig. 3d). None of the interventions, however, were complete; this is likely to reflect inter-individual variance in the effects of FNM, as we found a correlation of the FNM effect size for both ketamine and cocaine in a given individual (Fig. 3e).

Fast off-kinetics and NMDAR antagonism

We next screened for a form of synaptic plasticity that appears within hours after the first injection of an addictive drug[16] by testing for the presence of Ca^{2+}-permeable AMPARs in VTA dopamine neurons. Ketamine did not induce the inward rectification that is typical of the presence of such non-canonical AMPARs—in contrast to cocaine (Fig. 3f,g). To parse the temporal requirement for the induction of plasticity, we performed optogenetic activation of dopamine neurons in vivo for periods of increasing duration (Fig. 3h). Although 15 min of stimulation left the synapses unchanged, we found that 60 min of stimulation increased the rectification index (Fig. 3i), similar to the 2 h of stimulation reported previously[18]. This explains why, in the case of intraperitoneal injection of ketamine, activation of dopamine neurons for only a few minutes (Fig. 2b) was insufficient to induce plasticity.

The previous results suggest that the duration of dopamine neuron activation is a crucial predictor for the synaptic plasticity that is induced by 'drugs of abuse'. Next, therefore, we investigated what would happen if ketamine acted on dopamine neurons for a longer period, by repeatedly injecting ketamine. To generate such a drug regimen, we intravenously infused ketamine or cocaine every 2 or 4 min (based on self-administration; Extended Data Fig. 1d; ketamine 1 mg per kg per infusion, cocaine 0.75 mg per kg per infusion) for 2 h to generate an increase in the levels of dopamine in the NAc of comparable magnitude and duration for the two drugs (Fig. 3j,k). Although for cocaine this protocol increased the rectification index at excitatory synapses onto VTA dopamine neurons, this effect was not observed for ketamine (Fig. 3l). An additional mechanism may thus be involved to explain the lack of effect of ketamine on synaptic plasticity. This could be ketamine antagonizing NMDARs because, in addition to an increase in dopamine, the activation of NMDARs is required for the potentiation of excitatory synapses onto VTA dopamine neurons as well as D1R-MSNs[26]. Indeed, in patch-clamp experiments, application of

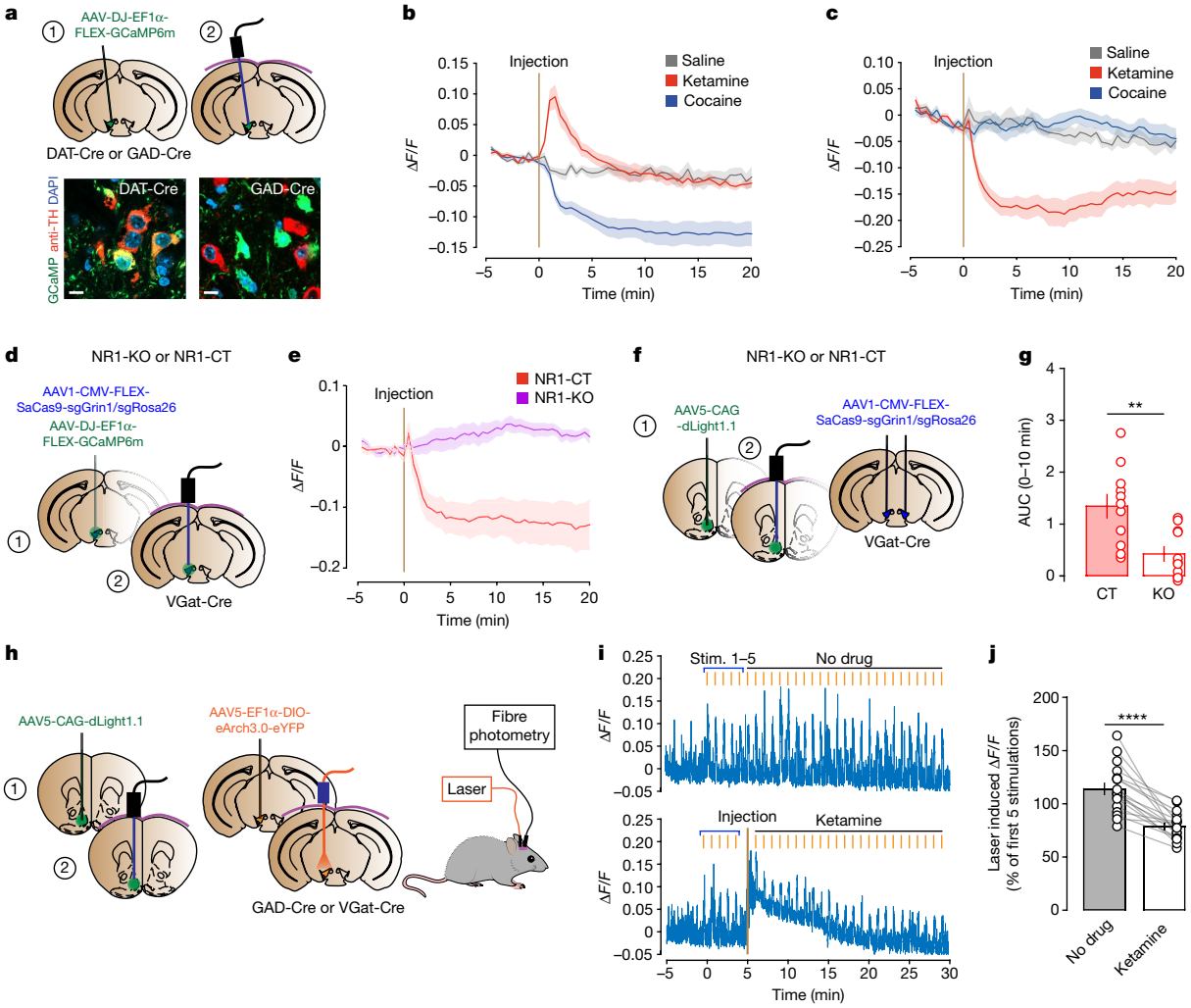

Fig. 2 | Accumbal dopamine transients are mediated by disinhibition of VTA dopamine neurons. a, Top, schematic of virus injection and fibre implantation. Bottom, GCaMP6m expression (green) and tyrosine hydroxylase (TH) immunostaining (red). Scale bars, 10 µm. **b**, Mean Ca^{2+} signal in VTA dopamine neurons with i.p. injections of saline, ketamine (30 mg kg^{-1}) and cocaine (15 mg kg^{-1}). $n = 10$ mice. **c**, Mean Ca^{2+} signal in VTA GABA neurons with i.p. injections. $n = 7$ mice. **d**,**f**,**h**, Experimental details. **e**, Mean Ca^{2+} signal in VTA GABA neurons from NR1-control (CT) and NR1-KO mice with i.p. injections of ketamine. n (mice) = 8 (CT) and 8 (KO). **g**, AUC of ketamine-induced dopamine transients in NR1-CT and NR1-KO mice. n (mice) = 11 (CT) and 11 (KO). **i**, Representative dLight responses to eArch3.0 stimulation from sessions without ketamine (top) and with ketamine (45 mg kg^{-1} i.p.; bottom). **j**, $\Delta F/F$ during eArch3.0 stimulation normalized to the first five trials. $n = 18$ mice. Data are mean ± s.e.m. $^{**}P < 0.01$, $^{****}P < 0.0001$.

ketamine at a concentration (50 µM) that corresponds to the expected levels in the brain in mice[27–29] strongly inhibited NMDAR-mediated synaptic currents (Extended Data Fig. 5). As a result, ketamine also blocked long-term potentiation in acute brain slices (Fig. 3m). Thus, in repeated drug application regimens in which the rapid off-kinetics of ketamine-induced dopamine effects are overcome, ketamine's NMDAR antagonism still prevents the induction of synaptic plasticity that is typically observed with addictive drugs.

No accumbal drug-evoked plasticity

As increased expression of FOS in NAc D1-MSNs is an early indication for drug-evoked plasticity[30–32], we quantified the levels of FOS after a single injection of ketamine. Unlike cocaine, there was no increase of FOS-positive D1-MSNs with ketamine (Fig. 4a–c). We next tested for locomotor sensitization as an early drug-adaptive behaviour. We injected mice for five days, followed by withdrawal and re-exposure. For the initial four to five daily injections we observed a short-term sensitization for ketamine and cocaine (Fig. 4d–f). However, when tested after 7 and 30 days of withdrawal, ketamine yielded a locomotor response that was similar to baseline, whereas sensitization persisted in mice that were treated with cocaine (Fig. 4d–f). In a separate cohort, after 14 days of withdrawal, no drug-evoked synaptic plasticity was observed with ketamine, as the rectification index and AMPA/NMDA ratio were comparable to those in saline-treated mice (Fig. 4g–i). By contrast, but in line with previous reports[33,34], cocaine increased the rectification index at medial prefrontal cortex (mPFC)-to-NAc D1-MSN synapses, whereas the AMPA/NMDA ratio decreased (Fig. 4g–i). In an attempt to test for addiction criteria that are typically reached by only a subset of self-administering mice[35], we allowed for daily four-hour-long access to ketamine, increasing the lever press ratio (fixed ratio; FR) every four days. Although this confirmed the reinforcing nature of ketamine (Fig. 1d), we observed that mice reduced self-administration once FR2 was introduced (Fig. 4j,k). When compared to self-administration of cocaine, the number of infusions and active lever presses for ketamine was lower (Fig. 4j, k). As a consequence, the break point in a progressive ratio schedule was also lower than what we observed with cocaine (Fig. 4l), speaking to the low motivation for ketamine self-administration. The sporadic lever presses at the end of the schedule were readily suppressed by the introduction of aversive

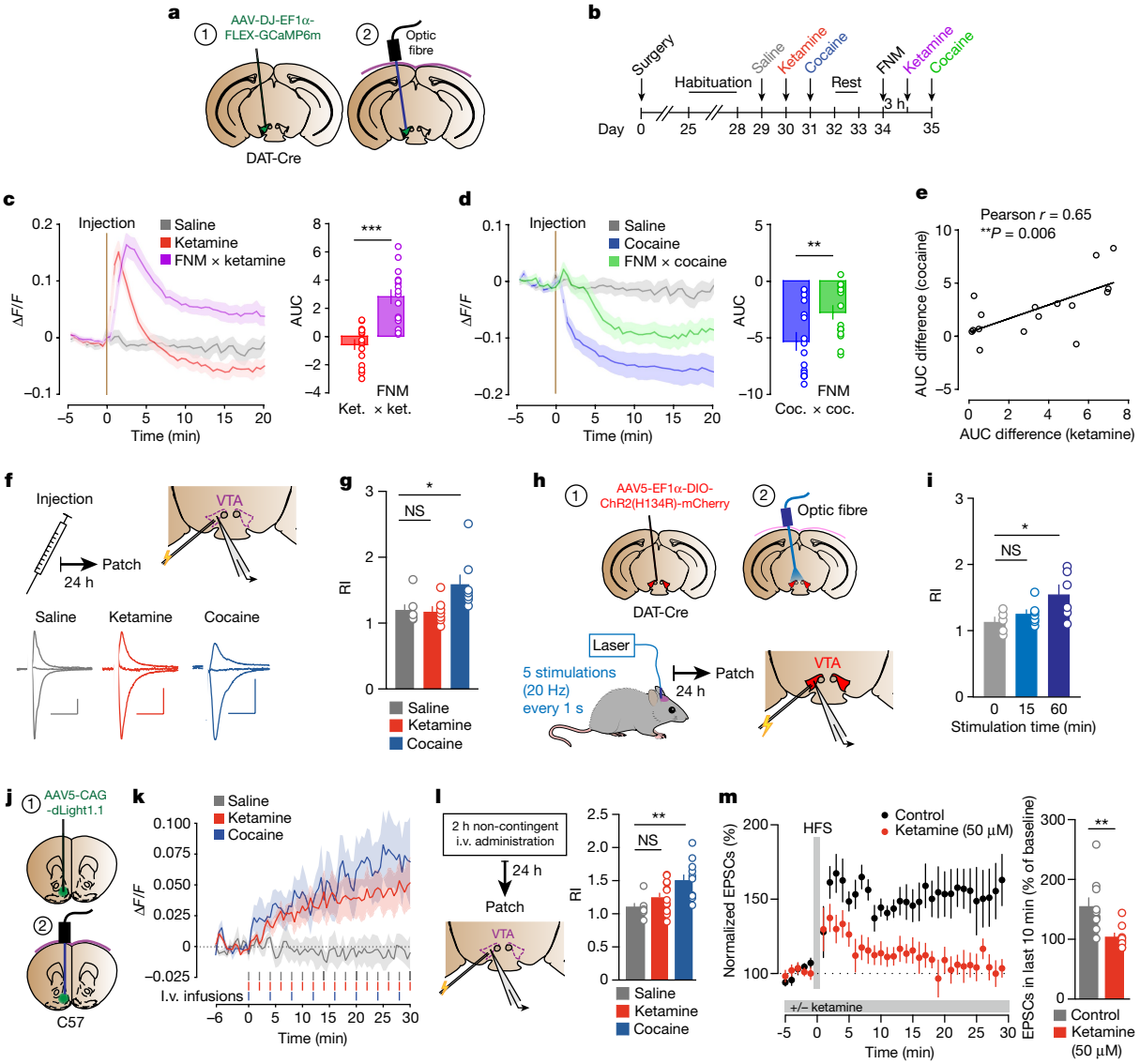

Fig. 3 | D_2R-mediated fast off-kinetics of dopamine transients and lack of early adaptive synaptic plasticity. a,**b**,**h**,**j**, Experimental details. **c**, Left, mean Ca^{2+} signal in VTA dopamine neurons with i.p. injections of saline, ketamine (30 mg kg^{-1}) and FNM (10 mg kg^{-1}) × ketamine. Right, AUC of ketamine-induced signal without and with pre-treatment with FNM. $n = 16$ mice. **d**, Left, mean Ca^{2+} signal in VTA dopamine neurons with i.p. injections of saline, cocaine (15 mg kg^{-1}) and FNM × cocaine. Right, AUC of cocaine-induced signal without and with FNM pre-treatment. $n = 16$ mice. The saline trace is the same as in **c** because conditions were assessed consecutively (**b**). **e**, Differences of AUC between cocaine-induced and FNM × cocaine-induced signal as a function of differences of AUC between ketamine-induced and FNM × ketamine-induced signal. **f**, Top, experimental details. Bottom, example traces of AMPAR currents used to calculate the rectification index (RI). Scale bars, 10 ms, 100 pA. **g**, RI of putative VTA dopamine neurons. n (cells) = 7 (saline), 7 (ketamine) and 8 (cocaine). **i**, RI in VTA dopamine neurons. n (cells) = 5 (0 min), 7 (15 min) and 7 (60 min). **k**, Mean NAc dLight response to intravenous (i.v.) infusions of saline and ketamine (1 mg per kg per infusion) every 2 min and cocaine (0.75 mg per kg per infusion) every 4 min. n (mice) = 4 (saline), 7 (ketamine) and 7 (cocaine). **l**, Left, experimental details. Right, RI in putative VTA dopamine neurons. n (cells) = 7 (saline), 13 (ketamine) and 11 (cocaine). **m**, Long-term potentiation induced in NAc slices with high-frequency stimulation (HFS). Left, time course of normalized excitatory postsynaptic currents (EPSCs) with and without 50 μM ketamine. Right, normalized EPSCs averaged across the last 10 min. n (cells) = 10 (control) and 8 (ketamine). Data are mean ± s.e.m. $^*P < 0.05$, $^{**}P < 0.01$, $^{***}P < 0.001$. NS, not significant.

air-puffs (Extended Data Fig. 6a). Air-puffs were chosen because of the slight analgesic effect of ketamine (Extended Data Fig. 6b). These experiments highlight the absence of ketamine-evoked synaptic plasticity, and show that ketamine does not induce long-term locomotor sensitization or uncontrolled self-administration despite initial reinforcing effects.

Discussion

Here we show that sub-anaesthetic doses of ketamine increase the activity of VTA dopamine neurons by inhibiting NMDARs in VTA GABA neurons. This elicits a dopamine transient in the NAc that is terminated within minutes because D_2Rs become activated. Like cocaine, ketamine reinforces initial self-administration. However, unlike cocaine, ketamine does not evoke drug-adaptive synaptic plasticity, long-term locomotor sensitization or uncontrolled self-administration. We argue that D_2R-mediated rapid off-kinetics and NMDAR antagonism preclude the potentiation of excitatory synapses in the VTA and NAc, thus limiting addiction liability.

The disinhibitory action of ketamine is reminiscent of the mechanism of action of opioids[25], benzodiazepines[36], γ-hydroxybutyrate (GHB)[37] and cannabinoids[38], which also inhibit VTA GABA interneurons. Ketamine is, however, unique in that the decrease of VTA GABA activity is

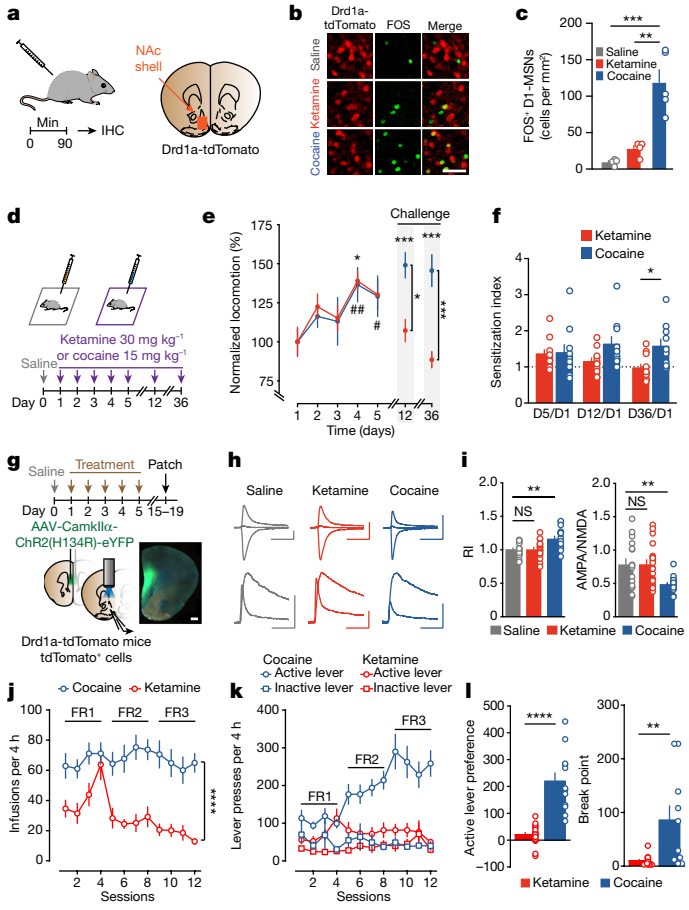

Fig. 4 | Absence of accumbal drug-evoked synaptic plasticity, locomotor sensitization and uncontrolled self-administration. a, Left, experimental timeline. Right, brain area for imaging. IHC, immunohistochemistry. **b**, Representative confocal images of NAc shell-expressing FOS. White arrows point to D1-MSNs expressing FOS. Scale bar, 50 µm. **c**, Average cell density per mouse for $FOS^+tdTomato^+$ cells in the NAc shell. *n* (mice) = 4 (ketamine), 5 (cocaine) and 4 (saline). **d**, Paradigm for locomotor sensitization. **e**, Distance travelled after i.p. injection, normalized to the first day of drug administration. *n* (mice) = 11 (ketamine) and 10 (cocaine). **f**, Sensitization index calculated for day 5 (D5/D1), day 21 (D12/D1) and day 36 (D36/D1). *n* (mice) = 11 (ketamine) and 10 (cocaine). **g**, Experimental details. Bottom right image: green, ChR2 infection site; orange, $tdTomato^+$ D1-MSNs; blue, DAPI. Scale bar, 500 µm. **h**, Example traces for RI (top) and AMPA/NMDA (bottom). Scale bars, 50 ms, 100 pA. **i**, Left, RI; right: AMPA/NMDA ratio in NAc D1-MSNs. For RI: *n* (cells) = 16 (saline), 18 (ketamine) and 16 (cocaine). For AMPA/NMDA: *n* (cells) = 16 (saline), 19 (ketamine) and 17 (cocaine). **j**, Number of ketamine (1 mg per kg per infusion) and cocaine (0.5 mg per kg per infusion) infusions during acquisition. *n* (mice) = 20 (ketamine) and 12 (cocaine). **k**, Left, number of active and inactive lever presses during ketamine and cocaine self-administration across sessions. Right, preference for active lever (active minus inactive lever presses) on the last session. *n* (mice) = 20 (ketamine) and 12 (cocaine). **l**, Break points of ketamine and cocaine self-administration. *n* (mice) = 20 (ketamine) and 10 (cocaine). Values are presented as mean ± s.e.m. $^{\#}P < 0.05$, $^{\#\#}P < 0.01$, $^{*}P < 0.05$, $^{**}P < 0.01$, $^{***}P < 0.001$, $^{****}P < 0.0001$. For all i.p. injections, doses were 30 mg kg^{-1} ketamine and 15 mg kg^{-1} cocaine.

caused by the loss of NMDAR excitation. As in interneurons elsewhere, NMDARs on VTA GABA neurons contribute to excitatory transmission at resting potential, maybe through receptors of non-canonical subunit composition[39]. A similar disinhibitory motif has been proposed in the mPFC, in which ketamine also inhibits GABA interneurons, such that the activity of pyramidal cells is disinhibited[40,41]. The activity of dopamine neurons is terminated by D_2Rs[42], which activate the G-protein-gated inwardly rectifying potassium (GIRK) family of ion channels, thus hyperpolarizing VTA dopamine neurons[43]. This could be a direct effect, as ketamine has been shown to act as a D_2R agonist with an inhibition constant (K_i; defined by [^{3}H]raclopride) of 0.5 µM (ref. [42], but see also ref. [44]). Alternatively, it could be the consequence of dendritic release of dopamine, as is the case with cocaine[23]. However, fentanyl-induced release of dopamine—which also occurs through disinhibition—has slower off-kinetics than ketamine. This difference would suggest a direct action of ketamine on D_2Rs, which remains controversial.

Many forms of drug-evoked synaptic plasticity require NMDARs for induction[45]. Moreover, there is hierarchical organization as plasticity in the VTA[16] is permissive for plasticity in the NAc[1,21] and eventually in the dorsal striatum[22]. Early drug-adaptive synaptic plasticity underlies drug seeking[33], compulsive drug use[22] and locomotor sensitization[34]. With ketamine, we observed neither synaptic plasticity in the mesolimbic dopamine system nor long-term locomotor sensitization. This is in line with previous reports of some degree of short-term sensitization[46,47]. Early forms of drug-evoked plasticity are necessary to engage the circuit organizations that eventually underlie compulsive drug seeking and drug taking[15]. As our data indicate the absence of uncontrolled ketamine self-administration, this strongly suggests that the addiction liability of ketamine is low.

The lack of drug-evoked synaptic plasticity has two reasons. First, with a single dose, because of its fast off-kinetics, the increase in dopamine was insufficient to cause plasticity in the VTA. Second, with repeated intravenous infusions that cause a longer-lasting increase in dopamine, NMDAR blockade prevented plasticity. The dual action that we have revealed here is relevant for therapy in humans. To treat depression, ketamine or its enantiomer esketamine are administered in sub-anaesthetic doses either as a 40-min intravenous infusion[48] (0.5 mg kg^{-1}) or as a nasal spray (esketamine; 56–84 mg) on a bi-weekly basis. As the nasal spray causes an acute exposure to ketamine that is similar to the intraperitoneal injections in our animal model, the fast off-kinetics of accumbal dopamine in combination with NMDAR blockade may preclude drug-evoked synaptic plasticity. Even with repetitive intravenous infusions that cause prolonged enhanced levels of dopamine, NMDAR blockade may still confine drug-adaptive plasticity.

Overall, we found that ketamine has rewarding and reinforcing properties as it indirectly acts on the dopamine system through circuit effects from local GABA neurons. The absence of drug-adaptive synaptic plasticity in the mesolimbic system strongly indicates that ketamine's addiction liability is limited by its pharmacology, as D_2R-mediated inhibition of dopamine neurons in the VTA explains the fast off-kinetics and NMDAR antagonism prevents induction mechanisms for synaptic changes. The insight that we provide here into the acute and chronic effects of ketamine on the mesolimbic dopamine system may help to provide a consensus on access to treatment for depression.

Online content

Any methods, additional references, Nature Research reporting summaries, source data, extended data, supplementary information, acknowledgements, peer review information; details of author contributions and competing interests; and statements of data and code availability are available at https://doi.org/10.1038/s41586-022-04993-7.

1. Bellone, C., Loureiro, M. & Luscher, C. Drug-evoked synaptic plasticity of excitatory transmission in the ventral tegmental area. *Cold Spring Harb. Perspect. Med.* **11**, a039701 (2021).
2. Di Chiara, G. et al. Dopamine and drug addiction: the nucleus accumbens shell connection. *Neuropharmacology* **47**, 227–241 (2004).
3. Lüscher, C., Robbins, T. W. & Everitt, B. J. The transition to compulsion in addiction. *Nat. Rev. Neurosci.* **21**, 247–263 (2020).
4. Lüscher, C. & Ungless, M. A. The mechanistic classification of addictive drugs. *PLoS Med.* **3**, e437 (2006).

5. Franks, N. P. & Lieb, W. R. Molecular and cellular mechanisms of general anaesthesia. *Nature* **367**, 607–614 (1994).
6. Zanos, P. et al. Ketamine and ketamine metabolite pharmacology: insights into therapeutic mechanisms. *Pharmacol. Rev.* **70**, 621–660 (2018).
7. Masuzawa, M. et al. Pentobarbital inhibits ketamine-induced dopamine release in the rat nucleus accumbens: a microdialysis study. *Anesth. Analg.* **96**, 148–152 (2003).
8. Witkin, J. M. et al. The rapidly acting antidepressant ketamine and the mGlu2/3 receptor antagonist LY341495 rapidly engage dopaminergic mood circuits. *J. Pharmacol. Exp. Ther.* **358**, 71–82 (2016).
9. Littlewood, C. L. et al. Mapping the central effects of ketamine in the rat using pharmacological MRI. *Psychopharmacology* **186**, 64–81 (2006).
10. Rocha, B. A., Ward, A. S., Egilmez, Y., Lytle, D. A. & Emmett-Oglesby, M. W. Tolerance to the discriminative stimulus and reinforcing effects of ketamine. *Behav. Pharmacol.* **7**, 160–168 (1996).
11. De Luca, M. T. & Badiani, A. Ketamine self-administration in the rat: evidence for a critical role of setting. *Psychopharmacology* **214**, 549–556 (2011).
12. Zanos, P. et al. A negative allosteric modulator for alpha5 subunit-containing GABA receptors exerts a rapid and persistent antidepressant-like action without the side effects of the NMDA receptor antagonist ketamine in mice. *eNeuro* **4**, ENEURO.0285-16.2017 (2017).
13. Suzuki, T. et al. Effects of the non-competitive NMDA receptor antagonist ketamine on morphine-induced place preference in mice. *Life Sci.* **67**, 383–389 (2000).
14. Luscher, C. & Malenka, R. C. Drug-evoked synaptic plasticity in addiction: from molecular changes to circuit remodeling. *Neuron* **69**, 650–663 (2011).
15. Luscher, C. The emergence of a circuit model for addiction. *Annu. Rev. Neurosci.* **39**, 257–276 (2016).
16. Ungless, M. A., Whistler, J. L., Malenka, R. C. & Bonci, A. Single cocaine exposure in vivo induces long-term potentiation in dopamine neurons. *Nature* **411**, 583–587 (2001).
17. Bellone, C. & Luscher, C. Cocaine triggered AMPA receptor redistribution is reversed in vivo by mGluR-dependent long-term depression. *Nat. Neurosci.* **9**, 636–641 (2006).
18. Brown, M. T. et al. Drug-driven AMPA receptor redistribution mimicked by selective dopamine neuron stimulation. *PLoS One* **5**, e15870 (2010).
19. Conrad, K. L. et al. Formation of accumbens GluR2-lacking AMPA receptors mediates incubation of cocaine craving. *Nature* **454**, 118–121 (2008).
20. Kourrich, S., Rothwell, P. E., Klug, J. R. & Thomas, M. J. Cocaine experience controls bidirectional synaptic plasticity in the nucleus accumbens. *J. Neurosci.* **27**, 7921–7928 (2007).
21. Mameli, M. et al. Cocaine-evoked synaptic plasticity: persistence in the VTA triggers adaptations in the NAc. *Nat. Neurosci.* **12**, 1036–1041 (2009).
22. Pascoli, V. et al. Stochastic synaptic plasticity underlying compulsion in a model of addiction. *Nature* **564**, 366–371 (2018).
23. Brodie, M. S. & Dunwiddie, T. V. Cocaine effects in the ventral tegmental area: evidence for an indirect dopaminergic mechanism of action. *Naunyn Schmiedebergs Arch. Pharmacol.* **342**, 660–665 (1990).
24. Hunker, A. C. et al. Conditional single vector CRISPR/SaCas9 viruses for efficient mutagenesis in the adult mouse nervous system. *Cell Rep.* **30**, 4303–4316 (2020).
25. Corre, J. et al. Dopamine neurons projecting to medial shell of the nucleus accumbens drive heroin reinforcement. *eLife* **7**, e39945 (2018).
26. Luscher, C. & Malenka, R. C. NMDA receptor-dependent long-term potentiation and long-term depression (LTP/LTD). *Cold Spring Harb. Perspect. Biol.* **4**, a005710 (2012).
27. Zanos, P. et al. NMDAR inhibition-independent antidepressant actions of ketamine metabolites. *Nature* **533**, 481–486 (2016).
28. Ganguly, S., Panetta, J. C., Roberts, J. K. & Schuetz, E. G. Ketamine pharmacokinetics and pharmacodynamics are altered by P-glycoprotein and breast cancer resistance protein efflux transporters in mice. *Drug Metab. Dispos.* **46**, 1014–1022 (2018).
29. Saland, S. K. & Kabbaj, M. Sex differences in the pharmacokinetics of low-dose ketamine in plasma and brain of male and female rats. *J. Pharmacol. Exp. Ther.* **367**, 393–404 (2018).
30. Valjent, E. et al. Involvement of the extracellular signal-regulated kinase cascade for cocaine-rewarding properties. *J. Neurosci.* **20**, 8701–8709 (2000).
31. Valjent, E. et al. Regulation of a protein phosphatase cascade allows convergent dopamine and glutamate signals to activate ERK in the striatum. *Proc. Natl Acad. Sci. USA* **102**, 491–496 (2005).
32. Bertran-Gonzalez, J. et al. Opposing patterns of signaling activation in dopamine D_1 and D_2 receptor-expressing striatal neurons in response to cocaine and haloperidol. *J. Neurosci.* **28**, 5671–5685 (2008).
33. Pascoli, V. et al. Contrasting forms of cocaine-evoked plasticity control components of relapse. *Nature* **509**, 459–464 (2014).
34. Pascoli, V., Turiault, M. & Luscher, C. Reversal of cocaine-evoked synaptic potentiation resets drug-induced adaptive behaviour. *Nature* **481**, 71–75 (2012).
35. Deroche-Gamonet, V., Belin, D. & Piazza, P. V. Evidence for addiction-like behavior in the rat. *Science* **305**, 1014–1017 (2004).
36. Tan, K. R. et al. Neural bases for addictive properties of benzodiazepines. *Nature* **463**, 769–774 (2010).
37. Cruz, H. G. et al. Bi-directional effects of $GABA_B$ receptor agonists on the mesolimbic dopamine system. *Nat. Neurosci.* **7**, 153–159 (2004).
38. Melis, M. et al. Endocannabinoids mediate presynaptic inhibition of glutamatergic transmission in rat ventral tegmental area dopamine neurons through activation of CB1 receptors. *J. Neurosci.* **24**, 53–62 (2004).
39. Paoletti, P., Bellone, C. & Zhou, Q. NMDA receptor subunit diversity: impact on receptor properties, synaptic plasticity and disease. *Nat. Rev. Neurosci.* **14**, 383–400 (2013).
40. Moghaddam, B., Adams, B., Verma, A. & Daly, D. Activation of glutamatergic neurotransmission by ketamine: a novel step in the pathway from NMDA receptor blockade to dopaminergic and cognitive disruptions associated with the prefrontal cortex. *J. Neurosci.* **17**, 2921–2927 (1997).
41. Ali, F. et al. Ketamine disinhibits dendrites and enhances calcium signals in prefrontal dendritic spines. *Nat. Commun.* **11**, 72 (2020).
42. Kapur, S. & Seeman, P. NMDA receptor antagonists ketamine and PCP have direct effects on the dopamine D_2 and serotonin 5-HT_2 receptors—implications for models of schizophrenia. *Mol. Psychiatry* **7**, 837–844 (2002).
43. Luscher, C. & Slesinger, P. A. Emerging roles for G protein-gated inwardly rectifying potassium (GIRK) channels in health and disease. *Nat. Rev. Neurosci.* **11**, 301–315 (2010).
44. Can, A. et al. Effects of ketamine and ketamine metabolites on evoked striatal dopamine release, dopamine receptors, and monoamine transporters. *J. Pharmacol. Exp. Ther.* **359**, 159–170 (2016).
45. Engblom, D. et al. Glutamate receptors on dopamine neurons control the persistence of cocaine seeking. *Neuron* **59**, 497–508 (2008).
46. Uchihashi, Y., Kuribara, H., Morita, T. & Fujita, T. The repeated administration of ketamine induces an enhancement of its stimulant action in mice. *Jpn. J. Pharmacol.* **61**, 149–151 (1993).
47. Wiley, J. L., Evans, R. L., Grainger, D. B. & Nicholson, K. L. Age-dependent differences in sensitivity and sensitization to cannabinoids and 'club drugs' in male adolescent and adult rats. *Addict. Biol.* **13**, 277–286 (2008).
48. Berman, R. M. et al. Antidepressant effects of ketamine in depressed patients. *Biol. Psychiatry* **47**, 351–354 (2000).

Methods

Mice

C57BL/6J (wild-type) mice were purchased from Charles River. Drd1-Tomato (Tg(Drd1a-tdTomato)6Calak/J), DAT-Cre (Slc6a3tm1.1(cre) Bkmn), GAD-Cre (Gad2tm2(cre)Z) and VGat-Cre (Slc32a1tm2(cre) Lowl/J) mouse lines were from The Jackson Laboratory. Male and female mice aged 3–20 weeks were used and housed with food and water ad libitum on a normal 12-h light–dark cycle (light on at 07:00) with temperature (18–23 °C) and humidity (40–60%) precisely controlled. Mice were group housed except for those used for self-administration experiments. All procedures were approved by the Institutional Animal Care and Use Committee of the University of Geneva and by the animal welfare committee of the Canton of Geneva, in accordance with Swiss law.

Drugs

A racemic mixture of ketamine was purchased as a 50 mg ml^{-1} solution from Labatec (Switzerland). Cocaine hydrochloride was provided by the pharmacy of the University Hospital of Geneva. Fentanyl was purchased as a 0.05 mg ml^{-1} solution from Sintetica (Switzerland). FNM (fluphenazine-*N*-2-chloroethane·2HCl) was from Enzo Life Sciences (Switzerland). For in vivo administration, ketamine and fentanyl solution were diluted with sterile 0.9% NaCl (saline). Cocaine and FNM were dissolved in saline. For intravenous (i.v.) administration, drug solutions were filtered (0.22 μm pore size).

Acute hyperlocomotion and behavioural sensitization

Mice were habituated to the behaviour room, handling and intraperitoneal (i.p.) injections on three days before testing. On testing days, mice underwent room habituation for a minimum of 1 h. Then, they were individually transferred into a testing arena (20 cm × 20-cm-squared box made of frosted opal-white acrylic glass). After 20 min of habituation to the arena, mice were i.p. injected and left in the arena for another 60 min. I.p. injections were saline (10 ml kg^{-1}), ketamine (30 mg kg^{-1}) or cocaine (15 mg kg^{-1}). For behavioural sensitization, injections (saline, ketamine or cocaine) were repeated daily for a total of 5 days. Drug challenge after home-cage withdrawal was tested after 7 and 30 days of withdrawal. Mice that were used for ex vivo patch-clamp experiments after sensitization underwent 10–14 days of withdrawal and were euthanized for slice recordings instead of getting exposed to a drug challenge behavioural session. Locomotor activity was recorded and analysed using ANY-maze v.4.95 (Stoelting). Sensitization index was calculated as total distance travelled in 30 min post-injection after sensitization divided by the distance on day 1 of drug administration.

Drug self-administration

Jugular vein catheters were implanted under anaesthesia with a ketamine and xylazine mixture (80 mg kg^{-1} and 10 mg kg^{-1}, respectively) one week before starting the experiment. After surgery, mice were singly housed and treated with the antibiotic amikacin (10 mg kg^{-1} subcutaneously) for 5 days. Catheters were flushed daily with heparin (2.5 international units) after the surgery, before and after the self-administration sessions until the end of the experiment.

Mice were mildly food-deprived for one night before the first self-administration session to increase exploratory behaviour. Ad libitum feeding resumed immediately after the first session. For the acquisition sessions, mice were placed individually into operant boxes with an active and an inactive lever (assignment counter-balanced between mice) and trained on a fixed ratio (FR) 1 schedule for Fig. 1c–e (first self-administration cohort), and increased FRs for Fig. 4j–l (second self-administration cohort). A press on the active lever turned on a cue light for 10 s (1-s on–off at 1 Hz) and the infusion of the assigned drug. There was a 20-s time-out after every infusion, during which lever pressing did not trigger any response. Infusions were ketamine (1 mg per kg per infusion), cocaine (0.75 mg per kg per infusion for Fig. 1c–e, and 0.5 mg per kg per infusion for Fig. 4j–l) or saline (1 ml per kg per infusion). For the first self-administration cohort, sessions lasted a maximum of 120 min or were terminated earlier when 45 infusions were administered (short access). For the second self-administration cohort, sessions lasted for 240 min (long access). After long-access sessions to ketamine, mice were subjected to two baseline and three punishment sessions, with each session lasting for 120 min. For punishment sessions, 1-s air-puffs (from two sides and above the mouse head) were conducted every three infusions. The experimental protocols were controlled and data were collected with MED-PC IV 4.34 (Med Associates).

Hotplate test

The mice were placed on the pre-heated (55 ± 0.2 °C) hotplate apparatus 0.5–1 h before and immediately after i.v. infusions of saline or ketamine (1 mg per kg per infusion, 4-min interval, 30 infusions within 2 h). Latency to hotplate was calculated as the time between placing the mice and the first jump, hind paw withdrawal, lick or tremble. A 30 s cut-off was set to avoid tissue damage.

Stereotactic surgeries

Standard stereotactic surgeries were conducted under isoflurane anaesthesia. GCaMP6m was from Stanford University vector core, dLight1.1 was from Addgene, and the NR1-KO and control viruses were provided by L. Zweifel[24]. All other viruses were purchased from the University of North Carolina vector core. Bregma and dura mater were used as reference points.

For the dLight experiments, AAV5-CAG-dLight1.1 (500 nl) was injected unilaterally at +1.5 anteroposterior (AP), ±0.7 mediolateral (ML) and −4.3 dorsoventral (DV) (NAc). For the GCaMP experiments, AAV-DJ-EF1α-FLEX-GCaMP6m (500 nl) was injected at −3.2 AP, ±0.6 ML and −4.5 DV (VTA).

For cell-specific NR1-KO and the respective control, 300 nl AAV1-CMV-FLEX-SaCas9-U6-sgGrin1 or AAV1-CMV-FLEX-SaCas9-U6-sgRosa26 were injected as an 8:1 mixture with AAV1-FLEX-EGFP-KASH at −3.2 AP, ±0.6 ML and −4.5 DV (VTA). The KASH virus was omitted for the KO experiments with GCamp6m recording in the VTA. The CRISPR–Cas9 virus (plasmid available from Addgene) and guide RNA were generated and validated in detail in a previous study[24]. In brief, a loxp-flanked *SaCas9* and a guide RNA under U6 promotor were inserted in the same vector. The guide RNA sequence was designed to target the most common exon of the gene according to online resources. The absence of the GluN1 subunit was confirmed by sequencing after fluorescence-activated cell sorting and by a lack of NMDA currents in infected cells[24].

For inhibition of VTA GABA cells, AAV5-Ef1α-DIO-eArch3.0-eYFP (300 nl) was injected unilaterally at −3.2 AP, ±0.6 ML and −4.5 DV (VTA). Optic fibres were implanted unilaterally 0.2–0.3 mm more dorsal than virus injections, and fixed in head caps with dental cement and anchor screws.

For patch-clamp experiments, AAV5-CamKIIα-ChR2(H134R)-eYFP (400 nl) was injected bilaterally at +1.9 AP, ±0.3 ML and −2.0 DV (mPFC). For in vivo stimulation of dopamine neurons, AAV5-Ef1α-DIO-ChR2(H134R)-mCherry (500 nl) was injected at −3.2 AP, ±0.9 ML and −4.5 DV with a 10° angle (VTA). An optic fibre was implanted at −3.2 AP, ±0.9 ML and −4.3 DV with a 10° angle.

Fibre photometry

Fibre photometry experiments were performed as before[25]. Specifically, mice were habituated to the testing room, handling and i.p. injections for five days before testing. For testing, mice were connected to the fibre photometry cable and placed in a circular arena (20 cm diameter) for 10 min of habituation. Then, 5 min of baseline fluorescence was recorded, followed by an i.p. injection of drug or saline and another 20–30 min of recording.

Specific experimental condition. FNM (10 mg kg^{-1} i.p.) was injected 3 h before ketamine. For VTA GABA neuron inhibition in the absence of drugs, a 5-min baseline was recorded, then an orange laser (593 nm, 10–15 mW) was turned on for 10 s every 1 min for 30 stimuli. For VTA GABA neuron inhibition in the presence of ketamine, a 5-min baseline was recorded, then five 10-s laser stimuli were delivered, the ketamine (45 mg kg^{-1}) was i.p. injected and the first of 25 laser stimuli was started 60 s after i.p. injection. For data analysis of VTA GABA inhibition, traces were aligned to the onset of laser with a 10-s baseline. $\Delta F/F$ values from the 10 s of baseline and 10 s during laser on were averaged, then the amplitude was calculated by subtracting the baseline fluorescence from the laser-on fluorescence. Eventually the stimulation amplitudes of the first five stimuli were averaged as well as stimuli 6–30, and the latter was normalized to stimuli 1–5.

Fibre photometry conditions. Fluorescent indicators were excited from two excitation sources, corresponding to 470 nm wavelength and 405 nm wavelength LED light (M470F3, M405FP1, Thorlabs). Excitation light was sinusoidally modulated and passed through excitation filters (FMC4_AE(405)_E(450-490)_F(500-550)_S) and onto an optic fibre patch cable (MFP_400/430/1100–0.48_4 m_FC-ZF2.5, Doric Lenses). The fibre patch cable was then connected to the chronically implanted optic fibre (MFC_400/430-0.48_6mm_ZF2.5(G)_FLT, Doric Lenses). Emission light travelled back through the same system, where it was filtered (500–550 nm wavelength) and acquired through a photoreceiver (Newport 2151). After pre-amplification by the photoreceiver (2×10^{10} V/A) the signal was digitized, demodulated and stored using a signal processor (RZ5P, Tucker Davis Technologies). Fibre photometry data were collected with TDT Synapse v.84 (Tucker Davis), analysed using MATLABR2016b (MathWorks). First, for the time before drug injection, the signal originating from the 405-nm excitation source was linearly regressed to the signal originating from the 470-nm excitation source. The regression coefficients are then applied to the entire 405-nm originating signal, scaling it to the 470-nm originating signal. $\Delta F/F$ was then computed as (470 nm signal − fitted 405 nm signal)/fitted 405 nm signal. Finally the $\Delta F/F$ was binned into appropriate time bins in the graphs and analyses.

In vivo stimulation of dopamine neurons

At 10–14 days after surgery, mice were tethered to an optic fibre in their home cage for 1 h. They received laser stimulation for 0, 15 or 60 min. Laser stimulation (473 nm, 15 mW, 4 ms pulse duration) was delivered in bursts of 5 pulses at 20 Hz every 1 s[18]. Mice were euthanized for patch-clamp recordings 24 h after stimulation.

Patch-clamp electrophysiology

For patch-clamp recordings, mice were euthanized and the brains were removed quickly. Brain slices of 220 µm thickness were cut in ice-cold artificial cerebrospinal fluid (aCSF; containing 119 mM NaCl, 11 mM D-glucose, 26.2 mM $NaHCO_3$, 2.5 mM KCl, 1.3 mM $MgCl_2$, 1 mM NaH_2PO_4 and 2.5 mM $CaCl_2$) and recovered for 15 min at 31 °C. For dopamine neurons, brains were cut in a cutting solution as described previously[49]. The internal solution for whole-cell patch-clamp contained 130 mM CsCl, 4 mM NaCl, 5 mM creatine phosphate, 2 mM $MgCl_2$, 2 mM Na_2ATP, 0.6 mM Na_3GTP, 1.1 mM EGTA, 5 mM HEPES, 5 mM QX-314 and 0.1 mM spermine, except for long-term potentiation (LTP) and NMDAR inhibition experiments, which were conducted with an internal solution containing 140 mM K-gluconate, 10 mM creatine phosphate, 2 mM $MgCl_2$, 5 mM KCl, 4 mM Na_2ATP, 0.3 mM Na_3GTP, 0.2 mM EGTA and 10 mM HEPES. Dopamine neurons were recorded with the same internal solution but without QX-314. Currents were evoked with blue light (470 nm LED, 1–4 ms pulse duration) or electrical stimulation (100 µs pulse duration) in the presence of 100 µM picrotoxin. Currents were amplified (Multiclamp 700B, Axon Instruments), filtered at 2.2 kHz and digitized at 20 kHz (National Instruments Board PCI-MIO-16E4, Igor, Wave Metrics). Data were collected with Igor 7 (Wave metrics). We did not correct for liquid junction potential (−3 mV). Cells were discarded if the series resistance changed by more than 20%.

For AMPA/NMDA ratios, recordings were performed at +40 mV holding potential without and with 2-amino-5-phosphonopentanoic acid (AP-5; 50 µM) to obtain isolated AMPAR currents and compute NMDAR currents from the combined AMPAR–NMDAR trace. For the rectification index, isolated AMPAR currents were recorded at −70, 0 and +40 mV. For NMDAR inhibition experiments, AMPARs were blocked with NBQX (10 µM) and Mg^{2+}-free aCSF was used. Dopamine cells were identified according to anatomical location, morphology and cell capacitance[49]. In the dopamine neuron stimulation experiment dopamine cells were identified by the presence of photocurrents.

For in vitro LTP experiments, NAc slices from wild-type mice were incubated in Mg^{2+}-free aCSF with or without 50 µM ketamine for 20–30 min, then recordings took place in normal aCSF (containing 10 µM SKF38393 and 100 µM picrotoxin) with or without 50 µM ketamine. LTP was induced with high-frequency stimulation (4 bursts of 100 stimuli at 100 Hz, 10 s between bursts) with depolarization to 0 mV holding potential.

For validation of GluN1 KO, AAV1-FLEX-EGFP-KASH was co-injected with AAV1-CMV-FLEX-SaCas9-U6-sgGrin1 to visualize GABA neurons and injection sites in the VTA. Whole-cell recordings were performed on EGFP-positive GABA neurons with picrotoxin (100 µM) in the bath. NMDA components were measured as currents 20 ms after the peak at +40 mV, and AMPA components were measured as the peak at −70 mV. Previous literature confirmed the absence of NMDA components without the obligatory GluN1 subunit[24,45,50].

FOS staining and immunohistochemistry

Drd1-Tomato mice were singly housed and habituated to handling and i.p. injections daily for seven days before the experiment. On the day of experiment, ketamine (30 mg kg^{-1}), cocaine (15 mg kg^{-1}) or saline (10 ml kg^{-1}) were i.p. injected, mice were put back in their home cages and 90 min after the injections they were transcardially perfused under deep pentobarbital (150 mg kg^{-1}, i.p.) anaesthesia. Brain sections were stained for FOS expression using standard immunohistochemistry. In brief, slices were incubated with primary antibody (1:5,000, rabbit polyclonal anti-FOS, Synaptic Systems, 226 003) for 36 h at 4 °C and a secondary antibody (1:500, Alexa 488 goat anti-rabbit, Invitrogen, A1108) was used for visualization. Cell nuclei were stained with Hoechst (1:1,000). Brain slices were imaged on a confocal microscope at 20× magnification and cells were counted manually by an experimenter blind to treatment.

Visualization of fibre location and protein expression

After fibre photometry experiments, mice were deeply anaesthetized with pentobarbital (150 mg kg^{-1}, i.p.) and transcardially perfused with 4% paraformaldehyde. Fixed brains were cut in 50-µm-thick slices and mounted on microscopy slides with mounting medium containing DAPI. In some cases, to visualize dLight expression or dopamine cells, we performed standard immunohistochemistry before slide mounting. In brief, slices were incubated with a primary antibody (1:500; for dLight: rabbit polyclonal anti-GFP, Invitrogen, A11122; for dopamine cells: mouse monoclonal anti-TH, Sigma, T2928) overnight at 4 °C and a secondary antibody (1:500, Alexa 488 goat anti-rabbit, Invitrogen, A1108 or Alexa 555 donkey anti-mouse, Invitrogen, A31570) was used for visualization. Cell nuclei in anti-GFP- or anti-TH-treated slices were stained with Hoechst (1:1,000), instead of DAPI.

Statistics and reproducibility

Data were analysed with Microsoft Excel 16.16.26 and GraphPad Prism 9. Sample size were estimated with G*power (HHU). Mice were randomly assigned to treatment conditions using an design of interleaved trials.

Data were analysed blind whenever possible. The experiments were replicated at least twice and were successfully reproduced. Data were tested for normal distribution using the Shapiro–Wilk normality test. Normally distributed datasets were then tested with parametric comparisons, whereas non-parametric tests were chosen for non-normally distributed datasets. Post-hoc comparison was conducted if ANOVA yielded a significant main effect or interaction. Comparisons were two-tailed. The number of experimental replicates is noted in the figure legends. Details of statistical tests are provided in Supplementary Table 1.

Reporting summary

Further information on research design is available in the Nature Research Reporting Summary linked to this paper.

Data availability

The datasets generated during and/or analysed during the current study are available in the Zenodo repository (https://doi.org/10.5281/zenodo.5772449)[51].

Code availability

The MATLAB code used for analysing the fibre photometry raw data is available in the Zenodo repository (https://doi.org/10.5281/zenodo.5772449).

49. Bariselli, S. et al. Role of VTA dopamine neurons and neuroligin 3 in sociability traits related to nonfamiliar conspecific interaction. *Nat. Commun.* **9**, 3173 (2018).
50. Zweifel, L. S., Argilli, E., Bonci, A. & Palmiter, R. D. Role of NMDA receptors in dopamine neurons for plasticity and addictive behaviors. *Neuron* **59**, 486–496 (2008).
51. Simmler, L. D. et al. Dual-action of ketamine confines addiction liability. *Zenodo* https://doi.org/10.5281/zenodo.5772449 (2022).

Acknowledgements We thank J. Cand for laboratory assistance and L. Zweifel for providing the conditional NR1-KO and control viruses. We thank A. Kwan, C. Bellone and M. Mameli for their comments on an earlier version of the manuscript. This study was supported by the Swiss National Science Foundation (L.D.S., grant number PZ00P3_174178; C.L., 310030_189188) and the European Research Council (AdG F-Addict).

Author contributions L.D.S. conceived the experiments and performed patch recordings, fibre photometry and behavioural experiments. Y.L. performed fibre photometry, patch recordings and behavioural experiments. L.C.H. performed immunohistochemistry, fibre photometry and behavioural experiments. A.H. performed mice surgeries and behavioural experiments. R.v.Z. performed fibre photometry experiments. L.D.S., Y.L., L.C.H. and R.v.Z. performed analyses. C.L., L.D.S. and Y.L. wrote the manuscript with the help of all authors. C.L. supervised the study.

Competing interests The authors declare no competing interests.

Additional information

Supplementary information The online version contains supplementary material available at https://doi.org/10.1038/s41586-022-04993-7.

Correspondence and requests for materials should be addressed to Christian Lüscher.

Peer review information *Nature* thanks Jean-Antoine Girault and the other, anonymous, reviewer(s) for their contribution to the peer review of this work. Peer reviewer reports are available.

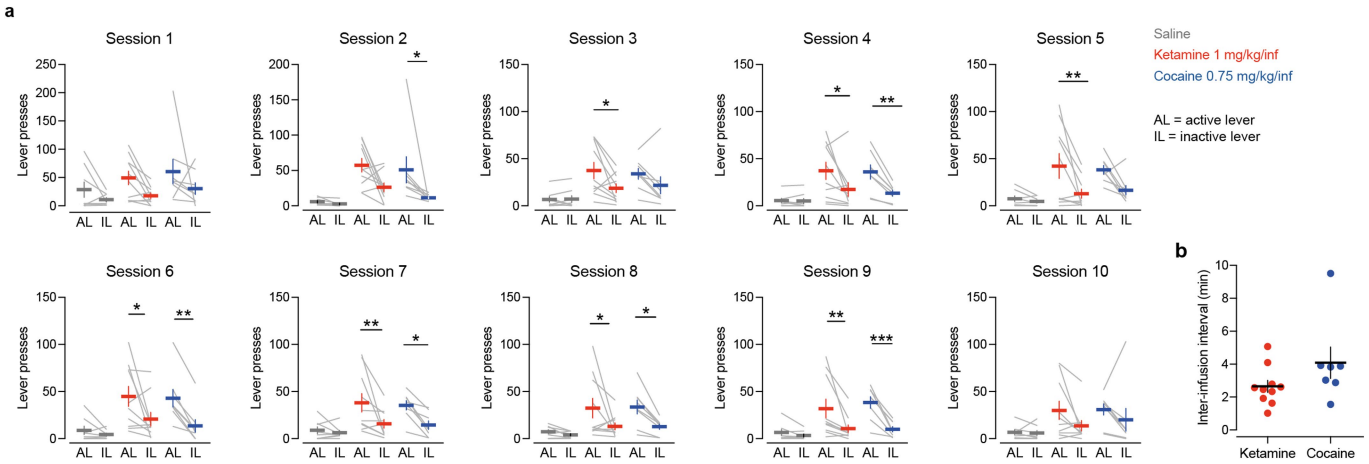

Extended Data Fig. 1 | Lever presses and infusion intervals of self-administration. a, Lever presses on active and inactive lever during self-administration for each session. *n* (mice) = 8 (saline), 10 (ketamine), 8 (cocaine). **b**, Median inter-infusion interval per mouse in session 6 to estimate rate of infusion during non-contingent self-administration (Fig. 3k). *n* (mice) = 10 (ketamine), 7 (cocaine). Data are represented as mean ± SEM. *P < 0.05, **P < 0.01, ***P < 0.001.

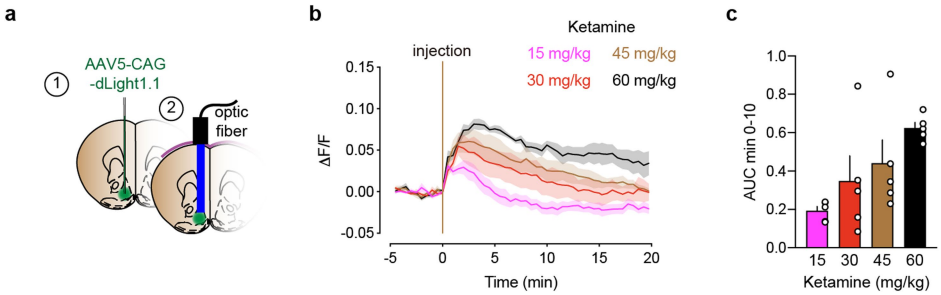

Extended Data Fig. 2 | Dose-dependence of accumbal dopamine transients. **a**, Schematic of virus injection and fibre implantation targeting the medial shell of the nucleus accumbens. **b**, Mean dLight response to i.p. injections of different doses of ketamine. $n = 5$ mice. **c**, AUC from 0–10 min after i.p. injection of different doses of ketamine. $n = 5$ mice. Data are represented as mean ± SEM.

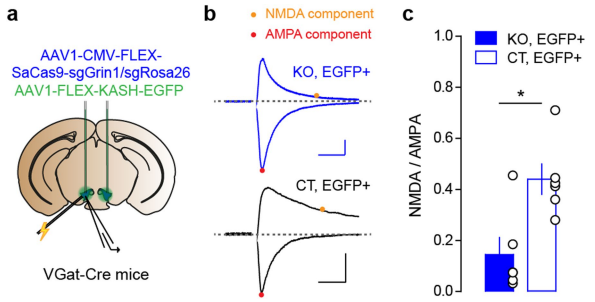

Extended Data Fig. 3 | Validation of NR1 ablation. a, Schematic of experimental details with virus injections and location of patch-clamp recordings. **b**, Representative traces of NMDA/AMPA recordings of NR1-KO (KO; sgGrin1) and control (CT; sgRosa26). Scale bar, 10 ms, 200 pA. **c**, NMDA/AMPA ratios (amplitudes measured for NMDA component 20 ms after the peak at +40 mV and AMPA component at −70 mV) of VTA GABA neurons from KO and CT mice. *n* (cells) = 6 (KO) and 6 (CT). Data are represented as mean ± SEM. *P < 0.05.

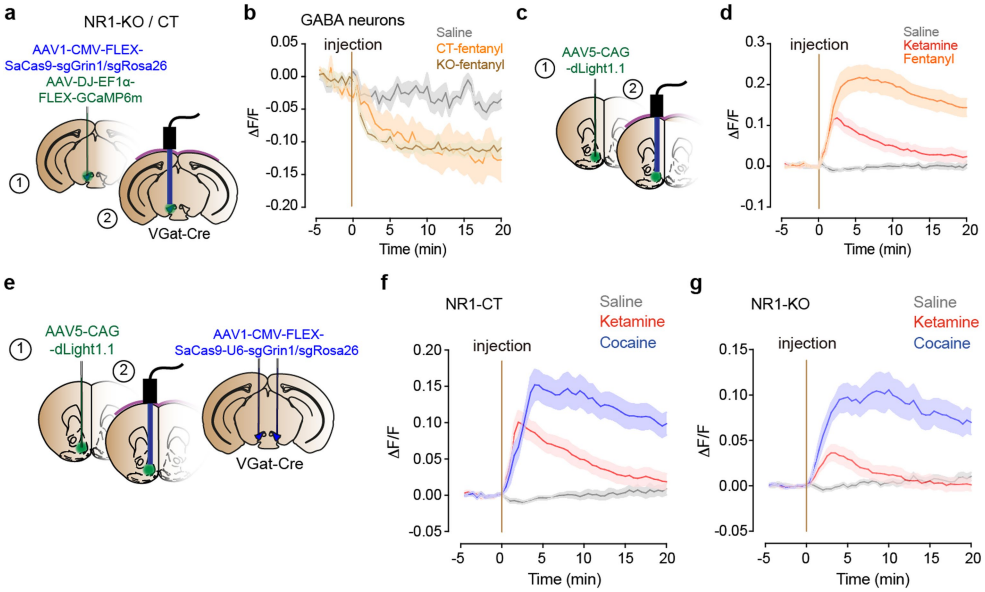

Extended Data Fig. 4 | Fentanyl- and ketamine-induced GABA inhibition and dopamine transients. a,**c**,**e**, Schematic of virus injection and fibre implantation. **b**, Mean Ca^{2+} signal of VTA GABA neurons from NR1-control (CT) and KO mice with i.p. injections of saline or fentanyl. *n* (mice) = 3 (CT) and 3 (KO). **d**, Average dopamine transients induced by ketamine (30 mg/kg) and fentanyl (0.3 mg/kg). *n* = 8 mice. **f**, Average dopamine transients induced by ketamine (30 mg/kg) and cocaine (15 mg/kg) in NR1-CT mice. *n* = 11 mice. **g**, Average dopamine transients induced by ketamine and cocaine in NR1-KO mice. *n* = 11 mice. Data are represented as mean ± SEM.

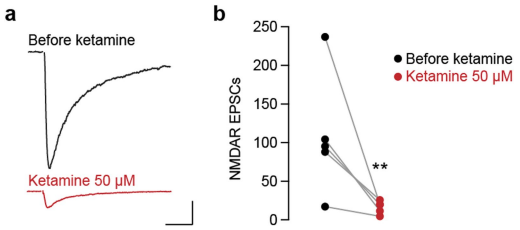

Extended Data Fig. 5 | In vitro NMDAR inhibition in acute brain slices of the NAc. a, Example traces of NMDAR EPSCs induced by electrical stimulation in the NAc, recorded in Mg^{2+}-free aCSF. Top: before bath-application of ketamine; bottom: with 50 µM ketamine. Stimulation artefact was removed. Scale bar is 50 ms, 50 pA. **b**, NMDAR EPSCs before and with ketamine. $n = 5$ cells. Data are presented as mean ± SEM. **P < 0.01.

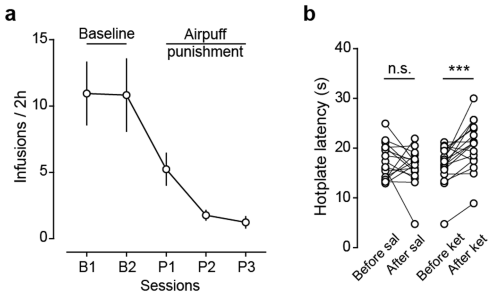

Extended Data Fig. 6 | Compulsive ketamine self-administration and pain perception affected by ketamine infusions. a. Number of ketamine infusions in baseline and punishment sessions. *n* = 17 mice. **b**. Latency to hotplate before and after mocked saline and ketamine i.v. infusions (1 mg/kg/infusion, 30 infusions). *n* (mice) = 16 (saline) and 17 (ketamine). Data are presented as mean ± SEM. ***P < 0.001.

nature portfolio

Corresponding author(s): Prof. Christian Lüscher

Last updated by author(s): May 24, 2022

Reporting Summary

Nature Portfolio wishes to improve the reproducibility of the work that we publish. This form provides structure for consistency and transparency in reporting. For further information on Nature Portfolio policies, see our Editorial Policies and the Editorial Policy Checklist.

Statistics

For all statistical analyses, confirm that the following items are present in the figure legend, table legend, main text, or Methods section.

n/a	Confirmed
☐	☒ The exact sample size (*n*) for each experimental group/condition, given as a discrete number and unit of measurement
☐	☒ A statement on whether measurements were taken from distinct samples or whether the same sample was measured repeatedly
☐	☒ The statistical test(s) used AND whether they are one- or two-sided *Only common tests should be described solely by name; describe more complex techniques in the Methods section.*
☐	☒ A description of all covariates tested
☐	☒ A description of any assumptions or corrections, such as tests of normality and adjustment for multiple comparisons
☐	☒ A full description of the statistical parameters including central tendency (e.g. means) or other basic estimates (e.g. regression coefficient) AND variation (e.g. standard deviation) or associated estimates of uncertainty (e.g. confidence intervals)
☐	☒ For null hypothesis testing, the test statistic (e.g. *F*, *t*, *r*) with confidence intervals, effect sizes, degrees of freedom and *P* value noted *Give P values as exact values whenever suitable.*
☒	☐ For Bayesian analysis, information on the choice of priors and Markov chain Monte Carlo settings
☒	☐ For hierarchical and complex designs, identification of the appropriate level for tests and full reporting of outcomes
☐	☒ Estimates of effect sizes (e.g. Cohen's *d*, Pearson's *r*), indicating how they were calculated

Our web collection on statistics for biologists contains articles on many of the points above.

Software and code

Policy information about availability of computer code

Data collection	Igor Pro 7, Wave metrics (Electrophysiology); MED-PC IV 4.34, Med Associates (self-administration); TDT synapse version 84, Tucker-Davis (fiber photometry); ANY-maze 4.95, Stoelting (Locomotor activity)
Data analysis	Matlab R2016b, Microsoft Excel 16.16.26, GraphPad Prism 9. Codes used for data analysis is available on Zenodo, doi: 10.5281/zenodo.5772449

For manuscripts utilizing custom algorithms or software that are central to the research but not yet described in published literature, software must be made available to editors and reviewers. We strongly encourage code deposition in a community repository (e.g. GitHub). See the Nature Portfolio guidelines for submitting code & software for further information.

Data

Policy information about availability of data

All manuscripts must include a data availability statement. This statement should provide the following information, where applicable:

- Accession codes, unique identifiers, or web links for publicly available datasets
- A description of any restrictions on data availability
- For clinical datasets or third party data, please ensure that the statement adheres to our policy

The datasets generated during and/or analyzed during the current study are available in the Zenodo repository, doi: 10.5281/zenodo.5772449.

Field-specific reporting

Please select the one below that is the best fit for your research. If you are not sure, read the appropriate sections before making your selection.

☒ Life sciences ☐ Behavioural & social sciences ☐ Ecological, evolutionary & environmental sciences

For a reference copy of the document with all sections, see nature.com/documents/nr-reporting-summary-flat.pdf

Life sciences study design

All studies must disclose on these points even when the disclosure is negative.

Sample size	Sample size were estimate with a power calculation software (G*Power).
Data exclusions	For patch-clamp recordings: cells with access resistance variance of > 20%. For fiber photometry: animals where injection and/or fiber implantation site were not correct.
Replication	Behavior, fiber photometry, staining experiments were replicated in 2 or more cohorts, conducted by 2-4 different experimenters. Patch clamp experiments were conducted by one or two different experimenters. All attempts at replication were successful.
Randomization	Mice were randomly assigned to treatment condition. Interleaved design was used for experimental conditions.
Blinding	Cell counting (c-Fos) was conducted by an experimenter blind to treatment. Fiber photometry, patch-clamp, behavior experiments were analyzed blind if applicable, but the experimenters are always aware of the conditions.

Reporting for specific materials, systems and methods

We require information from authors about some types of materials, experimental systems and methods used in many studies. Here, indicate whether each material, system or method listed is relevant to your study. If you are not sure if a list item applies to your research, read the appropriate section before selecting a response.

Materials & experimental systems

n/a	Involved in the study
☐	☒ Antibodies
☒	☐ Eukaryotic cell lines
☒	☐ Palaeontology and archaeology
☐	☒ Animals and other organisms
☒	☐ Human research participants
☒	☐ Clinical data
☒	☐ Dual use research of concern

Methods

n/a	Involved in the study
☒	☐ ChIP-seq
☒	☐ Flow cytometry
☒	☐ MRI-based neuroimaging

Antibodies

Antibodies used	Rabbit polyclonal anti-c-Fos Synaptic Systems 226 003; rabbit polyclonal anti-GFP Invitrogen A11122; mouse monoclonal anti-TH Sigma T2928, clone TH-16; Alexa 488 goat anti-rabbit Invitrogen A1108; Alexa 555 donkey anti-mouse Invitrogen A31570
Validation	All primary antibodies were suitable for IHC according to vendor. Anti-c-Fos antibody shows perfect results in immunostaining experiments like ICC, IHC and IHC-P according to the manufacturer's website. Anti-HT antibody stained selectively VTA and SNR in the midbrain in our hands. Anti-GFP antibody stained selectively in virus infected area in our hands, and was validated according to the manufacturer's website by obtaining positive staining in GFP ransfected in HEK-293E cells while no signal in non-transfected cells.

Animals and other organisms

Policy information about studies involving animals; ARRIVE guidelines recommended for reporting animal research

Laboratory animals	C57BL/6J (wildtype), Drd1-Tomato (Tg(Drd1a-tdTomato)6Calak/J), DAT-Cre (Slc6a3tm1.1(cre)Bkmn), GAD-Cre (Gad2tm2(cre)Z) and VGat-Cre (Slc32a1tm2(cre)Lowl/J) mice lines were used. For all strains, both male and female mice were used. For all strains, mice ages 10-20 weeks were used for in vivo experiments, ages 3-15 weeks were used for patch clamp recordings.
Wild animals	No wild animals were used in the study.
Field-collected samples	No field collected samples were used in the study.

Ethics oversight	All procedures were approved by the Institutional Animal Care and Use Committee of the University of Geneva and by the animal welfare committee of the Canton of Geneva, in accordance with Swiss law.

Note that full information on the approval of the study protocol must also be provided in the manuscript.